



Review—Metallic Lithium and the Reduction of Actinide Oxides

Augustus Merwin,^a Mark A. Williamson,^b James L. Willit,^b and Dev Chidambaram^{a,c,*}

^aMaterials Science and Engineering, University of Nevada, Reno, Nevada 89557, USA

^bNuclear Chemical Engineering Department, Nuclear Engineering Division, Argonne National Laboratory, Argonne, Illinois 60439, USA

^cNevada Institute for Sustainability, University of Nevada, Reno, Nevada 89557, USA

Extensive research and process development has been conducted on the electrolytic reduction of actinide oxides in molten LiCl-Li₂O. It is now accepted that the reduction of these metal oxides occurs via two separate reduction mechanisms: direct electro-chemical reduction and mediated chemical reduction by metallic lithium. The deposition of metallic lithium at the cathode (mediated chemical reduction mechanism) during the process is known to be essential in order to achieve high process throughputs and reduction yields, and yet a knowledge gap exists regarding the nature of metallic lithium in this system. This review summarizes the formation of lithium during the process and its dispersion into the molten salt electrolyte. Previously reported aspects of the physical chemistry of the LiCl-Li₂O-Li system are presented with a specific focus on the dispersion of Li in the solution. Finally, issues regarding the effect of the presence of lithium on the electrolytic reduction process are discussed. Evidence shows that electrochemically generated metallic lithium is likely a significant source of experimental uncertainty, low current efficiency and Li₂O consumption in the oxide reduction process.

© The Author(s) 2017. Published by ECS. This is an open access article distributed under the terms of the Creative Commons Attribution Non-Commercial No Derivatives 4.0 License (CC BY-NC-ND, <http://creativecommons.org/licenses/by-nc-nd/4.0/>), which permits non-commercial reuse, distribution, and reproduction in any medium, provided the original work is not changed in any way and is properly cited. For permission for commercial reuse, please email: oa@electrochem.org. [DOI: 10.1149/2.0251708jes] All rights reserved.



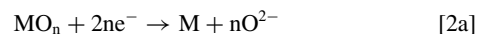
Manuscript submitted February 16, 2017; revised manuscript received April 24, 2017. Published June 6, 2017. *This paper is part of the JES Focus Issue on Progress in Molten Salts and Ionic Liquids.*

The reduction of uranium, plutonium and minor actinide oxides to a metallic form is an important nuclear fuel cycle process.²⁻⁹ The ability of metallic lithium to reduce various uranium oxides, importantly UO₂ and U₃O₈, has been known for many years.¹⁰ A molten salt metalthermic reduction process employing metallic lithium (Li) as a reductant dissolved in molten LiCl was first developed by Argonne National Laboratory (ANL) to consolidate a variety of forms of actinide oxides for integration into a single electrometallurgical reprocessing system.¹¹⁻¹³ An electrolytic process, often referred to as electro-deoxidation or simply oxide reduction, was subsequently developed as a more controllable method of reducing metal oxides. A feasibility study conducted by Poa et al. demonstrated that oxides of uranium and plutonium could be reduced electrochemically in molten salts as long as the reduction potential of the metal oxide in question was more noble than the cation of the electrolyte.^{14,15} This approach was further developed by Gourishankar et al. to better understand processes chemistry and develop the electrolytic cell technology.^{13,16-20} Independent research conducted by Fray, Farthing, and Chen (FFC) applied the principles of electrochemical reduction in molten salt electrolytes to a variety of metal oxide reduction processes.^{21,22} The FFC process has been the subject of several literature reviews.²³⁻²⁵ While these review articles address the processes associated with the reduction of nuclear fuel in LiCl, they focus on the electro-deoxidation phenomena and the CaCl₂-CaO system. Additionally, the process engineering of the electrolytic reduction of nuclear fuel, and experience in incorporating oxide fuel into pyroprocessing, has been the focus of a recent review article.²⁶ The current review will focus on the role metallic lithium plays in the electrolytic reduction of actinide oxides in LiCl-Li₂O.

The primary difference between the direct lithium reduction process and the electrolytic reduction process is that the molten salt used in the former begins as LiCl saturated with Li. During the reduction process, the oxide concentration in the salt increases up to its solubility limit of 11.6 mol% at 650°C as Reaction 1 progresses.²⁷⁻²⁹



Alternatively, in the electrolytic process, Li₂O is added as an oxide ion transport species intentionally, and its concentration remains constant throughout the process. In this process the reduction of the metal oxide, MO_x, occurs via Reaction 2a and oxygen gas is evolved at the anode via Reaction 2b.



The electrolytic process is a noted improvement compared to the direct lithium reduction method.^{13,17,19,20,30,31} In the latter process, the reaction between dissolved Li and the metal oxide is difficult to control under Li saturated conditions, especially at the surface of the melt due to the lower density of Li compared to LiCl. Corrosion of the container materials used to hold the electrolyte in the direct reduction process proved to be difficult due to the presence of reducing Li, and oxidizing LiCl. Additionally, the concentration of Li₂O in the melt cannot be controlled in the direct reduction process other than by controlling the oxide/salt ratio. In both processes, the concentration of Li₂O in the salt must be maintained below certain levels due to the decrease in the Gibbs free energy of reducing actinide oxides with increasing oxygen ion activity. Lithium reduction of PuO₂ and AmO₂ was demonstrated by Usami et al., however only at less than 3 and 1.8 wt% Li₂O in the melt, respectively.^{29,32} The electrolytic reduction process is highly advantageous in this respect, as the concentration of Li₂O, in theory, remains at a controlled level throughout the reduction process. The adaptation of the electrochemically driven reduction process has been highly successful, resulting in reduction yields exceeding 99%.³³

Electrolytic reduction in LiCl-Li₂O has been successfully used to reduce MOX, as well as simulated high burnup SIMFUEL.³⁴⁻³⁶ In a non-nuclear context, electrolytic reduction in LiCl-Li₂O has been adapted to TiO₂,³⁷ SiO₂,³⁸ Ta₂O₅³⁹ and Nb₂O₅.⁴⁰ The electrolytic reduction of actinide oxides in LiCl-Li₂O is unique compared to transition metal oxides in that the reduction potential of the primary components of interest, namely UO₂ and PuO₂, are so close to the reduction potential of Li₂O that the mechanisms of reduction are significantly more complex.

Due to the roughly 70 mV difference in reduction potential between UO₂ and Li₂O, electrolytic methodologies can theoretically be

*Electrochemical Society Member.

^zE-mail: dcc@unr.edu

employed in the reduction of nuclear fuel.^{41–43} Experience with the process has shown however, that in practice significant overpotential is required to achieve high process throughputs, and as a result a cell potential exceeding the Li₂O electrochemical window is required.^{30,44–48} Principle investigators at the Korean Atomic Energy Research Institute (KAERI),⁴⁸ Central Research Institute of Electric Power Industry (CRIEPI),⁴⁹ and the Idaho National Laboratory (INL)⁴⁷ have independently reported that the electrolytic reduction cell is operated with the cathode at a more cathodic potential than the lithium reduction potential, and that the reduction takes place via both the direct, and the electrochemical reduction mechanisms shown as Reactions 1 and 2, respectively.

It will be shown in the following review that significant quantities of metallic lithium form on the cathode during the reduction of actinide oxides. Despite its presence in the system, and the important role it plays in the reduction, the nature and chemical form of lithium in this process is not well understood. This review attempts to discuss the role of lithium in this process; both, how it is formed and how it interacts with the system, in an attempt to emphasize its critical importance in understanding the oxide reduction process.

Experience with the Reduction Process

Extensive fundamental research and engineering scale experience with the reduction of actinide oxides has yielded critical information regarding the mechanics of the process.^{30,44} The process fundamentals, adopted by virtually all researchers, are as follows: polarization between an inert anode material, usually platinum, and a stainless steel cathode basket containing the metal oxide to be reduced is conducted at a cell voltage of approximately 3 V in a molten bath of LiCl containing 0.5–3 wt%Li₂O at 650°C. Studies have demonstrated that optimal process conditions include a Li₂O concentration of 1–2 wt%, and a cathode to anode surface area ratio of 2.6.^{7,50} Research into the anodic behavior of platinum under these conditions has demonstrated that platinum can operate as a nearly inert anode if the concentration of Li₂O is maintained above 0.5 wt% and the anode potential is less than +2.6 V vs Li/Pb.⁵¹ If the activity of the O²⁻ ion decreases significantly, the dissolution of platinum occurs via Reaction 3. However, the anode corrodes via the formation of Li₂PtO₃, as shown in Reaction 4, if the anode potential is too high.^{50,51} Alternative anode materials have been proposed, however none have been widely adopted.^{48,52–59}



Sakamura et al. compared the electrolytic reduction of UO₂ in LiCl and CaCl₂ and found that experiments conducted in LiCl exhibited significantly superior current efficiencies and higher yields compared to those conducted in CaCl₂.⁶⁰ Metallic Ca was formed on the cathode during the polarization in CaCl₂, but it did not penetrate the exterior U metal that was reduced initially. It was observed that a dense metal surface formed on the exterior of the UO₂, which prevented the discharge of O²⁻ from the remaining oxide, inhibiting the continuation of the reduction process. As a result, UO₂ in the center of the fuel pellets was found to be not reduced. This effect has driven research in the electrolytic reduction of UO₂ to be conducted almost exclusively in LiCl-Li₂O.

Voloxidation of used nuclear fuels is considered as a head-end process prior to oxide reduction to separate the fuel from the cladding, remove volatile fission products, and to reduce the particle size of the fuel.^{61–64} Voloxidation is achieved by reacting nuclear fuel with an oxidizer, typically O₂ gas, at high temperature to promote the oxidation of UO₂ to U₃O₈. The removal of volatile and salt soluble fission products from the fuel by this process is desirable as it reduces the activity of the pyroprocessing electrolyte salts.⁶⁵ Reducing the particle size of the oxide fuel through voloxidation has been shown to increase the kinetics of the oxide reduction process.⁶⁶ However, research into the reduction behavior of U₃O₈ has shown that it reacts

to form lithium uranates, and reduces to UO₂ prior to reducing to metallic uranium.^{44,67,68} Furthermore, it has also been demonstrated the reduction of U₃O₈ to UO₂ occurs spontaneously upon exposure to molten LiCl-Li₂O.^{44,69} Therefore, because the reduction of U₃O₈ progresses via the reduction of UO₂, the reduction of the latter remains the primary energy barrier to the electrochemical process. The current review will focus on the reduction of UO₂ specifically, as the aspects that are demonstrated to occur during its reduction will inevitably occur during the reduction of U₃O₈.

Despite being capable of high reduction yields, the electrolytic reduction process is known to exhibit low current efficiencies and, in some instances, consume Li₂O. Table I shows reported process parameters associated with the reduction of UO₂ conducted by various organizations. For previously stated reasons, the reduction yields and current efficiencies reported for the reduction of U₃O₈ cannot be compared to those of UO₂, and are therefore omitted from the following discussion.

Table I demonstrates that no research to date has quantitatively demonstrated a current efficiency of greater than 66%. Additionally, it has to be demonstrated that the process kinetics and efficiency are deteriorated as the process proceeds due to the accumulation of soluble fission products in the electrolyte.⁴ These deleterious effects, associated primarily with the accumulation of KCl and CsCl in the LiCl-Li₂O, were attributed to a decrease in the solubility limit of Li₂O in the melt. Decreasing the transport of O²⁻ in the electrolyte suppresses the reaction kinetics by limiting Reaction 2b. Additionally, as demonstrated in Table I, multiple studies have reported the loss of measurable quantities of Li₂O during the process. Quantification of the consumption of Li₂O during the process is complicated due to the presence of Li in the electrolyte, for reasons that will be discussed subsequently. Furthermore, it has been demonstrated that oxides of salt soluble fission products, primarily Cs, Ba, Rb, and Sr, will react with LiCl to form their respective chlorides and Li₂O.^{4,30} By producing Li₂O, these reactions would result in an apparent rate of Li₂O consumption that is considerably lower than the true value. While the consumption of minor quantities of Li₂O may appear insignificant on a bench scale, the potential loss of large quantities during industrial scale operations is seen as a major process impediment.⁷⁷

The Formation of Li During the Electrolytic Reduction of UO₂

Preliminary attempts to avoid the reduction of Li⁺ during the reduction of actinide oxides employed limited currents to avoid the cathode from reaching the Li|Li⁺ reduction potential. Figure 1

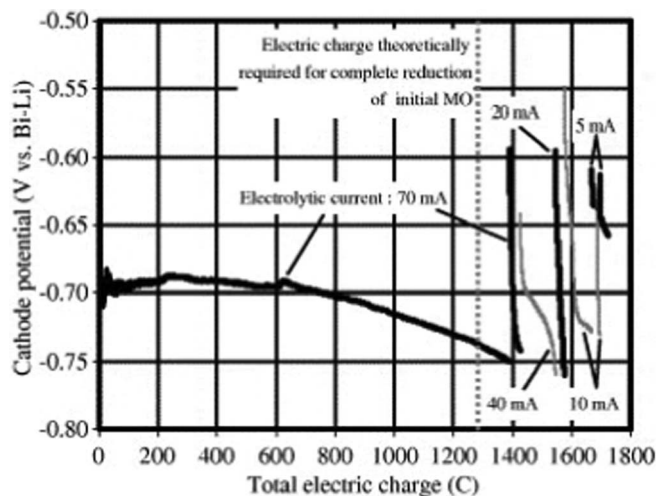


Figure 1. The cathode potential measured during galvanostatic polarization of (U-40Pu-5Np)O₂. The electrolysis was periodically interrupted after the cathode achieved the Li|Li⁺ potential at -0.75 V vs Bi/Li. Despite these attempts the Li|Li⁺ potential was rapidly re-established in each successive polarization.⁷⁸

Table I. Reported process parameters of the electrolytic reduction process.

Institution	Initial wt%Li ₂ O	Final wt%Li ₂ O	Charge Transfer (%)	Reduction Yield	Mass (g)	Reference	Comments
CRIEPI	-	-	150	Complete**	18	5	
CRIEPI	1	-	160	Complete**	103.5	70	Observed anode potential increase before adding 0.3wt%Li ₂ O
CRIEPI	-	-	135	99.2**	100	71	
KAERI	1	-	150	100	18	66	
KAERI	1.01	.97	150	>95	20	45	
KAERI*	1	0.89	200	100	5	72	
KAERI	1	0.98	150	98.9	20	73	
KAERI	1.37	-	177	98	17,000	7	Lost ~0.47wt%Li ₂ O in 12 hours before adding ~0.8wt%Li ₂ O
KAERI	1	-	150	88	4.1	35	
KAERI	1	-	170	99	29.7	74	
INL	1	-	220	99.7	50	75	Ended with anode potential increase (~0.5wt%Li ₂ O)
INL	1	0.8	150	67	50	47	
INL	1	-	263	98	50	42	Ended with anode potential increase (~0.5wt%Li ₂ O)
INL	1	-	220	99.7	45	76	Ended with anode potential increase (~0.5wt%Li ₂ O)

*Denotes the use of a LiCl-KCl-Li₂O electrolyte.

**Denotes reduction yield quantification based strictly on visual observation.

shows the cathode potential recorded as a function of current passed through the salt during the reduction of (U-40Pu-5Np)O₂ fuel in LiCl-0.51%Li₂O.⁷⁸ This investigation had intended to maintain a cell current of 70 mA, but was forced to reduce the current after exceeding the Li|Li⁺ potential of -0.75 V vs Bi/Li. The cell had to be interrupted after 108% of the theoretical charge was passed, a quantity recognized to be insufficient to result in significant reduction yields. After the initial interruption, each successive polarization approached the Li|Li⁺ potential more rapidly, indicating that the Li|Li⁺ potential had to be exceeded in order to achieve sufficient reduction yields.

Galvanostatic polarization of U₃O₈ at minimal current densities, as low as 26.5 mA/cm², resulted in a cathode potential more cathodic than the Li|Li⁺ reduction potential of -1.75 V vs Pt reference electrode after approximately 30% of the theoretical charge was passed through the cell.^{43,67} The authors further noted that following the reduction experiments, the cathode basket vigorously produced gas bubbles when rinsed in water; an observation they attributed to the presence of metallic lithium in and on the cathode. These two examples demonstrate that avoiding the Li|Li⁺ potential during the reduction process is impractical if the process is to be conducted at an industrially viable rate.

It should be noted that Li forms in the oxide reduction process at potentials more noble than the Li|Li⁺ standard potential. Li is soluble in LiCl at 650°C, and as a result it has an activity as solvated Li that is less than unity until the melt is saturated.^{1,79-83} Therefore, according to the Nernst equation, Li⁺ can be reduced at potentials more noble than the Li|Li⁺ standard potential as long as the activity of Li in the melt is not unity. This is important to note considering the proximity of the U|U⁴⁺ and Li|Li⁺ potentials. Li will form at the U|U⁴⁺ standard potential, however at an activity that is in accordance with the Nernst equation. For example, approximating the difference in the Li|Li⁺ and U|U⁴⁺ standard potentials as 70 mV, and taking the activity of Li⁺ as unity in the LiCl salt phase, Li will exist at an activity of 0.414 at the U|U⁴⁺ standard potential.

Recent approaches to the reduction process have employed potentiostatic polarization to maintain the cathode potential below the Li|Li⁺ potential, as opposed to the galvanostatic polarization previously discussed in which the cathode potential is not controlled. Figure 2c and 2e show electrical responses recorded during the re-

duction of SIMFUEL and of UO₂, reported by KAERI and INL, respectively.^{35,76,84} Cathodic cyclic voltammograms (CVs) conducted by the respective researchers are also included in Figure 2a and 2d for comparison.

The electrical circuit was periodically interrupted during the electrolytic reduction studies shown in Figure 2c and 2e to avoid the deposition of excessive quantities of Li and to monitor the open circuit potential (OCP) of the cathode assembly. It is important to note that, during these periods of cell interruption, the cathode OCP is observed to be the Li|Li⁺ potential demonstrated by the respective CV's shown in Figures 2a and 2d. This effect has been noted by numerous studies, and is attributed to the measurement of the OCP of metallic lithium existing on the cathode at unit activity.^{5,35,42,45,52,71-73,75,85,86} Due to the presence of Li on the cathode it can be concluded that the process proceeded via both Reactions 1 and 2. It is important to note that metallic lithium must be in physical contact with the cathode and the molten LiCl-Li₂O electrolyte in order for the electrochemical potential of the cathode to be measured at Li|Li⁺ potential.

Interpretations of electrode potentials made while passing current through the cell can lead to false conclusions due to ohmic potential drop effects. In any electrochemical process, the potentials measured by a power supply are skewed by voltage drops associated with iR losses in the electrochemical cell as well as the cabling between the power supply and the electrodes. This effect is largest in industrial processes employing large currents, where even resistances of a few ohms can result in potential drops on the order of the electrochemical effect under investigation. However, OCP measurements, such as those shown in Figures 2c and 2e, are not subjected to such effects. As a result, it is noted that OCP measurements provide more accurate information than electrode potentials made during cell operation.

Reduction of actinide oxides has also been achieved in molten LiCl-KCl-Li₂O.^{48,72} The electrical response of a reduction experiment conducted in LiCl-KCl-Li₂O is shown in Figure 3. It is observed that two separate cathode OCPs were recorded when the cell was interrupted, a fact that Hur et al. attributed to the measurement of the Li|Li⁺ and the K|K⁺ potentials at -1.27 V and -1.42 V vs Li-Pb, respectively.⁷² It is noted that the solubility of Li₂O in LiCl-KCl has been reported to be 4 mol% at 520°C,²⁸ less than half of the solubility

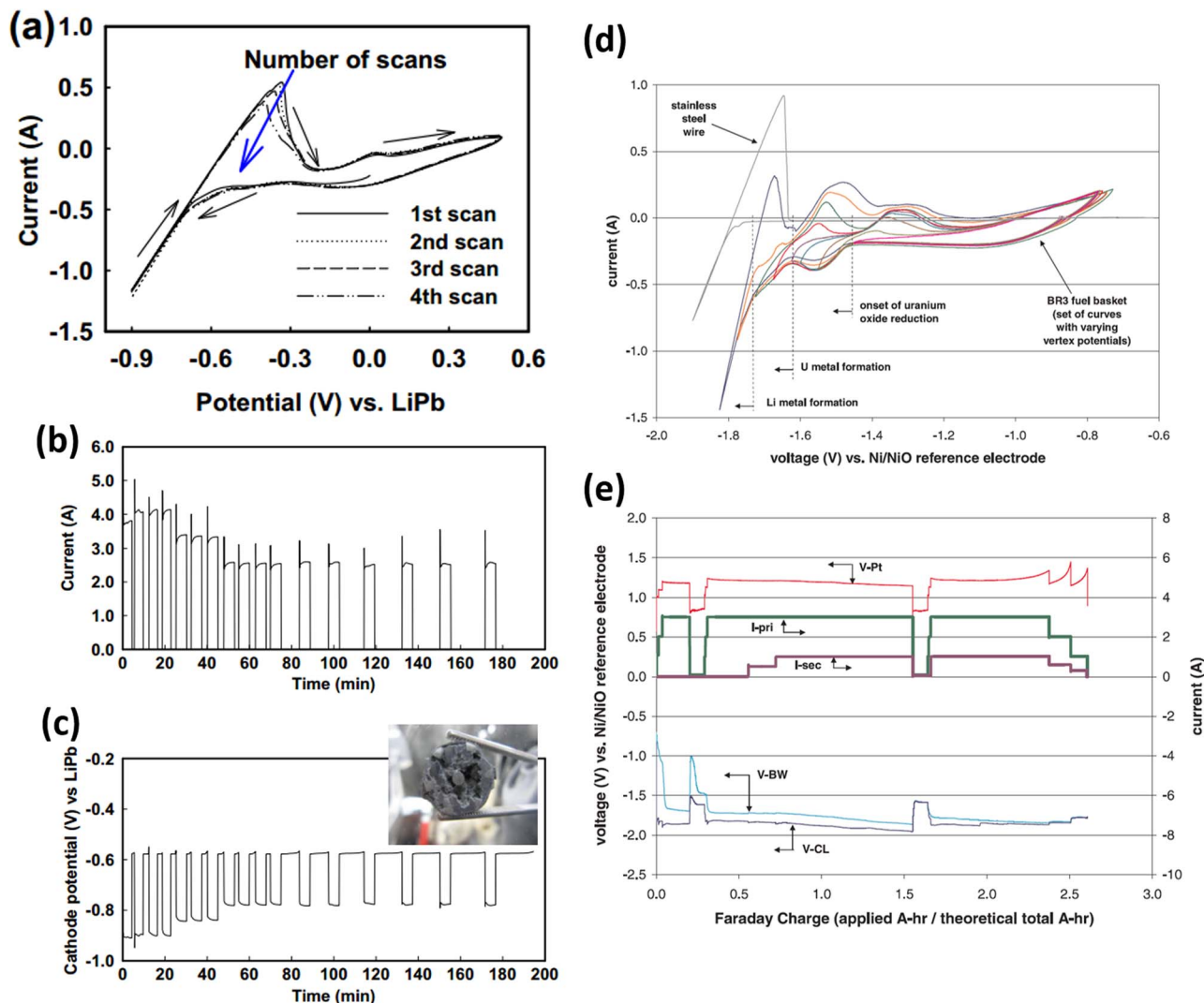


Figure 2. Electrical responses recorded during the reduction of SIMFUEL and UO_2 published by KAERI (left) and INL (right), respectively. (a) CV of SIMFUEL polarized vs a LiPb reference. (b) and (c) Cell current and cathode potentials recorded during the reduction of SIMFUEL. (d) CVs of a stainless steel wire and UO_2 polarized against a Pt reference. (e) Cell current and electrode potential responses recorded during the reduction of UO_2 . It is apparent in both studies that the OCP of the cathode is that of $\text{Li}|\text{Li}^+$ observed in the CV when the polarization is ceased.^{35,76}

in LiCl at 650°C .^{27–29} Therefore, the use of a LiCl-KCl electrolyte is expected to lower process kinetics by limiting Reaction 2b.

In research conducted by Choi et al. the electrical circuit was held open during the periods of cell interruptions as long as the cathode remained at the $\text{Li}|\text{Li}^+$ potential.³⁵ The departure from the $\text{Li}|\text{Li}^+$ potential is demonstrated by the gradual increase in cathode potential at the end of each cell interruption in Figure 2c. The length of time that the basket remains at the $\text{Li}|\text{Li}^+$ potential increases with polarization time; indicating that the time required for the activity of metallic lithium at the molten salt / cathode interface to dissipate increases as the process proceeds. There are two plausible ways for the metallic lithium phase to dissipate: by reacting with UO_2 through Reaction 1, or via dissolution into the salt. (Note that as reduction proceeds the reduced uranium metal shell on the feed material is in electrical contact with the cathode, effectively extending the cathode area across the fuel bed, albeit with a voltage drop across the bed due to iR .)

The kinetics of the oxide reduction process are known to be diffusion limited; as the reduction rate decreases asymptotically as the process progresses to completion.^{46,47,66,86} Recent modeling of the process employed a diffusion model using the production of Li at the cathode as the source term according to Faraday's law of electrolysis.⁴⁶ Interestingly, this model successfully fit numerous data sets by em-

ploying the direct reduction mechanism as the sole reduction pathway, neglecting the electro-deoxidation mechanism. It was reported that during the initial stages of reduction, the kinetics were limited by the production of Li due to the cell current; however, as the process proceeded toward completion, the diffusion through the exterior shell of metallic uranium limited the reaction kinetics.

The reduction process initiates with the rapid reduction of the exterior shell of each oxide particle, forming a porous metallic layer surrounding the oxide center. The process kinetics are then limited by two potential mechanisms; the diffusion of Li to the UO_2 , and the diffusion of the O^{2-} to the bulk electrolyte. Diffusion through the exterior metallic shell has been shown to be the rate limiting step in the process, due to the relatively rapid diffusion of the O^{2-} in the fluid salt phase.^{47,66} However, significant disagreement exists in the literature as to whether the process is limited by the diffusion of Li into, or O^{2-} out of, the pellet.^{4,35,46} The diffusion of Li^+ through the porous metallic phase is unlikely to occur without the prior reduction of Li^+ because the metallic phase is held below the $\text{Li}|\text{Li}^+$ potential. As a result of the oxide being incased in a metallic phase that is in electrical contact with the cathode held below the $\text{Li}|\text{Li}^+$ potential, the reduction of Li^+ is expected to occur at the metallic surface of the pellets. Once formed on the exterior of the metallic phase, Li can undergo

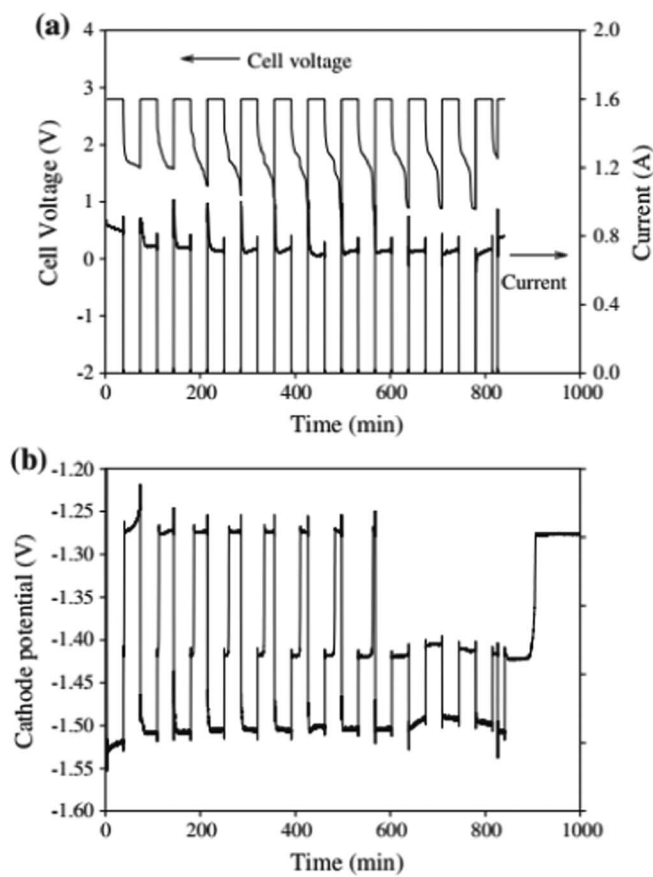


Figure 3. (a) Figure 3 Cell voltage, current and (b) cathode potentials measured during the reduction of UO_2 in $\text{LiCl-KCl-Li}_2\text{O}$ at 520°C using a LiPb reference electrode. The recording of both the $\text{K}|\text{K}^+$ and the $\text{Li}|\text{Li}^+$ potentials when the cell was interrupted demonstrates the presence of metallic K and Li on the cathode.⁷²

oxidation and lead to the reduction of U^{4+} . This process can occur nearly spontaneously because both phases are in physical contact with electrically conducting U metal. However, in order to conserve charge neutrality, this process is kinetically limited by the recombination of O^{2-} with the oxidized Li^+ . This results in the process reduction kinetics being limited by diffusion O^{2-} out of the pellet. Many authors have attributed observations of increased reduction kinetics to altering process variables that would result in increased O^{2-} transport out of the cathode assembly such as; decreasing the UO_2 pellet size, increasing the UO_2 porosity, rotating the cathode assembly, and changing the material of the cathode assembly.^{5,6,18,26,44,47,66,87,88} These observations strongly suggest that the diffusion of O^{2-} out of the oxide pellet, through the metal phase, is the rate limiting step of the electrolytic reduction process.

Physical Chemistry of $\text{LiCl-Li}_2\text{O-Li}$

Due to the previously discussed formation of metallic lithium during the reduction of actinide oxides, and the known solubility of Li in LiCl at 650°C , it can be concluded that metallic lithium dissolves into the electrolyte during the oxide reduction process.^{1,79-83} Considering the presence of Li in the molten $\text{LiCl-Li}_2\text{O}$ electrolyte, it is necessary to review aspects of fluid mixtures of metals and conjugate salts containing a cation of the same element. Bredig et al. were highly successful in classifying these mixtures into two categories, although it is important to emphasize that the two models are not mutually exclusive, and aspects of both have been observed simultaneously under non-ideal conditions.⁸⁹⁻⁹² The first model applies most directly to mixtures of alkali metals and alkali-halide salts, such as Na in

NaCl .^{79,93} These solutions are known to exhibit true, microscopically homogeneous, solution behavior in the salt rich region of the phase diagram, and rapidly change their physical properties with the inclusion of a minor quantity of metal.^{94,95} Such phases have been successfully described using an adapted version of the F^- center model of ionic crystals. In this model, the metallic atoms are treated as anion vacancies, replaced by an excess electron. A key indication of mixtures of this type is a sharp rise in electron mobility, with the inclusion of a small percentage of metal in the solution, demonstrating a transition from a nonmetallic to a metallic state. The second classification of metal-salt mixtures applies to more complicated systems, for example Bi in BiI_3 .^{89,96} In these mixtures, chemical interactions between the metal atoms and the salt anions results in the formation of abnormally reduced complexes referred to as subhalides. In such situations, the change in physical properties that accompanies the nonmetal-metal transition does not occur until much higher concentrations of metal are present in the mixture. The larger amount of metal required to induce this change is due to the consumption of excess electrons in the formation of the subhalides. The properties of the $\text{LiCl-Li}_2\text{O-Li}$ electrolyte will be discussed in the context of fitting into these two models.

Despite numerous investigations, the solubility limit of Li in molten LiCl is still widely debated.^{1,79-81,97,98} Initial investigations by Dworkin et al. at Oak Ridge National Laboratory (ORNL) measured the solubility limit using thermal analysis to be 0.5 ± 0.2 mol% at 640°C .⁷⁹ Researchers at ORNL were highly successful in developing phase diagrams of numerous metal-salt solutions, yet they noted exceptional difficulty in characterizing the LiCl-Li system.^{79,89,93,99-101} Attempts to characterize the electrical conductivity of LiCl-Li solutions, data that were used to support alternative metal-salt phase diagrams, were unsuccessful due to chemical reactions between Li and the crucibles. Park et al. reported the solubility limit of Li in LiCl to be 0.22 mol% at 650°C , however no reference to the experimental data supporting this conclusion could be found.³⁰

Simpson et al. have recently investigated the solubility of Li in $\text{LiCl-Li}_2\text{O}$ and discussed the difficulties associated with the chemical analysis of samples containing both Li_2O and Li.⁹⁸ These difficulties are highlighted later in this article. It was reported that Li concentrations in the range of 0.02 to 0.57 wt% (approximately 0.12 to 3.4 mol%) were observed, however a greater degree of confidence was reported for concentrations between 0.04 and 0.12 wt% (approximately 0.25 to 0.73 mol%). It was also noted that the solubility limit of Li was not highly affected by the concentration of Li_2O in the melt.

Nakajima et al. reported significantly different observations regarding the quantity of Li that could be dispersed in LiCl .^{1,82,83,102} In a series of experiments, metallic lithium was added in excess to one side of a U shaped container full of LiCl . The melt container was configured such that the Li floated on one end of the melt, while the container passed through a low point and raised on the other side where the salt was sampled. In this manner, the float of Li would not pass to the sampling region due to its lower density compared to LiCl . The quantity of lithium that was found to be dispersed in LiCl in these experiments was observed to be much higher in comparison to previous reports. Figure 4 shows the quantity of lithium observed in LiCl as a function of equilibration time, agitation time, as well as the concentration of Li_2O and Li_3N in the salt.

The concentrations of lithium observed to be dispersed in molten LiCl shown in Figure 4 depart from a general understanding of the electrolyte used in the oxide reduction process. Nakajima et al. hypothesized that the quantity of lithium per unit volume of molten LiCl was the sum of two different forms; true solution and colloidal suspension. The true (physical) solubility limit was reported as 0.66 mol%, a value within the margin of error reported by separate investigators.^{79,83} It is noted that the additional quantity of Li suspended in the molten salt in the form of a colloid would not be detectable in thermal analysis because the metallic lithium would not undergo a phase change during dispersion. The metal rich portion of the LiCl-Li system, if present, is not expected to contain large quantities of LiCl or O, as their solubility

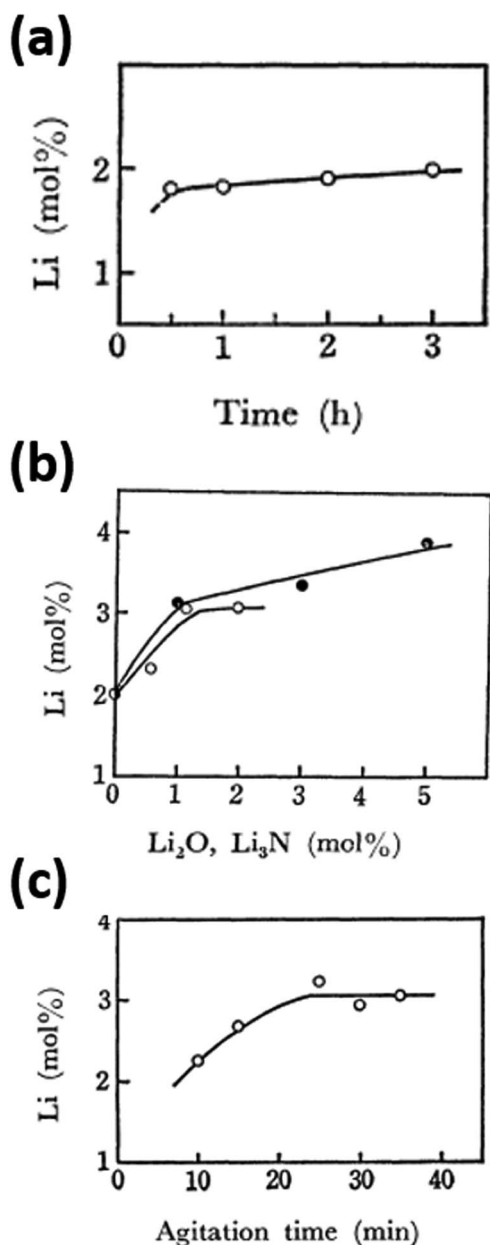


Figure 4. Measured concentrations of dispersed Li in molten LiCl as a function of (a) time in the absence of agitation (b) Li₂O and Li₃N concentration and (c) agitation time¹ (a) Concentration of lithium vs time in the absence of agitation. (b) Effects of lithium oxide and nitride on the lithium concentration at 650°C, agitation: 1000 rpm. ○ = Li₂O ● = Li₃N (c) Effect of agitation time on the lithium concentration at 650°C. Agitation: 1000 rpm with 1.4 mol%Li₂O added.

limits in liquid lithium are reported to be approximately 0.005 mol% and 2 mol%, respectively.^{103,104} Alternatively, the solubility limit of Li₂O is relatively high in LiCl at 11.6 mol% at 650°C.^{27–29}

Liu et al. investigated the seemingly anomalous behavior of the LiCl-Li system, and the reasons it behaved significantly differently compared to other alkali metal-alkali halide solutions.^{80,81} In these studies, the solubility of Li in LiCl was measured using potentiometry via observation of the electrochemical potential of a lithium deposit as it dispersed into solution. The solubility limit recorded using this technique was 1.8 mol% at 650°C. It should be noted that the salt used in this experiment was dried at 500°C prior to melting, and that no agitation was employed during the solubility measurements. These experimental parameters are important for characterizing unperturbed

molten LiCl-Li as opposed to melts that contain impurities or exist under forced convection. The solubility limit of 1.8 mol% is in agreement with data reported by Nakajima et al. in Figure 4a, and due to the nature of the experiment, appears to be representative of the total quantity of Li that disperses in LiCl in the absence of agitation. Two important facts were stated by Liu et al.: the observation that the thermodynamic activity of metallic Li is not unity when in contact with molten LiCl, and that an intermediate and momentarily stable electrochemical potential was observed between that of the lithium deposit and that of the bare electrode OCP.⁸¹ The first observation has significant implications regarding the Li|Li⁺ reduction potential and will be discussed later. The observation of an intermediate OCP, between the potentials of metallic lithium and the working electrode, was suggested as evidence of the formation of a lithium rich compound that was soluble in molten LiCl. This hypothesis proposes the formation of a Li_xCl compound with a value of X greater than one, in contrast to the accepted miscibility gap phase diagram behavior of alkali metal-alkali halide solutions proposed by Bredig.⁸⁹ The formation of an additional, subhalide, compound may be in agreement with the observation of the two seemingly different dissolution mechanisms previously discussed. Nakajima et al. attributed the dissolution of excessive quantities of lithium to the formation of suspended Li colloids, emulsified by impurity level quantities of Li₂O and Li₃N; however, it can be observed in Figure 4b that the amount of Li dispersed in LiCl was not highly dependent upon the concentration of either.¹ It is therefore reasonable to suggest that the quantity of dispersed lithium observed in these studies, up to 2–3 mol%, was present in the form of an unidentified complex or subhalide in addition to the quantity physically dissolved in the solution.

Héban et al. reached the conclusion that Li₂Cl is formed at the interface of molten lithium and eutectic LiCl-KCl salt.^{97,105} This research employed density functional theory (DFT) to determine the most thermodynamically stable subhalide possible in the molten LiCl-KCl-Li₂O-Li-K system, and subsequently used electrochemical techniques for experimental validation of this hypothesis. These reports noted that the formation of Li₂Cl was independent of the presence of KCl, and was detectable at the LiCl-Li interface, although experimental data was not provided. The presence of Li₂Cl as a subhalide in molten LiCl-Li₂O-Li suggests that the solution may be readily described by the second of Bredig's models.^{79,97,105}

In addition to being termed a subhalide, Li₂Cl can be classified as a hyperlithiated compound. Hyperlithiated compounds have been experimentally observed by several researchers and are of significant academic interest due to their apparent departure from the octet rule of quantum mechanics.^{106–108} Additionally, experimental observation of hyperlithiated oxygen, in the form of Li₃O and Li₄O has been reported, a fact that is potentially important to the LiCl-Li₂O-Li electrolyte in question.^{108–111} The role of Li₂O in the LiCl-Li₂O-Li system is largely unknown. It has been demonstrated that Li₂O dissociates nearly completely in LiCl, however how the O²⁻ ion interacts with Li is not yet understood.¹¹²

The electrical conductivity of the LiCl-Li system is exceedingly small compared to other metal-salt solutions, specifically the other alkali-alkali halides.^{80,92–94,113} This behavior has been attributed to the formation of a high population of bound F⁻ centers in the LiCl-Li system, as opposed to the loosely bound electrons that are more probable in alternative systems; for example Na-NaI. The low electrical conductivity of the LiCl-Li system is further evidence that the system is more adequately described by the more complicated model of metal-salt solutions where chemical interactions between the metal and salt result in the consumption of what would be free electrons, thereby suppressing electrical conductivity under metal saturated conditions. This conclusion was recently stated in a review of molten salt electrolytic processes by Masset et al.¹¹⁴ Similar conclusions were reached during the studying “metal fog” formed during the electrolysis of lithium from LiCl-KCl where authors stated: “The metal fog generated in the Li electrolysis with larger cathodic current is hardly explained by simple dissolution”.¹¹⁵ This report further hypothesized that the phenomena observed could be explained by

the formation of a salt soluble compound other than that of metallic lithium.

Recent research conducted in our laboratory has reported evidence that molten LiCl-Li, in the presence or absence of Li₂O, exhibits the Raman spectroscopic characteristics of the lithium nanoclusters Li₈.¹¹⁶ Should Li clusters be miscible with molten LiCl, a well-defined solubility limit of Li in LiCl may not exist due to the dispersion mechanism of colloidal suspension in addition to physical dissolution. In this case, the quantity of Li that may be suspended or dispersed under a given set of conditions would be highly dependent upon experimental factors such as thermally induced mixing of the melt or mechanical agitation. Furthermore, the presence of a second Li phase, in addition to bulk metallically bonded Li, would complicate the thermodynamics of the LiCl-Li system as each phase would possess separate activities. It is suggested that such effects are the cause of the previously unattributed physical properties of molten LiCl-Li.

In summary, it is suggested that the nature of the LiCl-Li₂O-Li electrolyte is likely a superposition of multiple dispersion phenomena, and does not fit exclusively into either of Bredig's models. While the true dissolution of ~0.5 mol% Li in LiCl may be successfully described by the F-center model, in accordance with alternative alkali-alkali halide solutions, the formation of subhalides and or dispersion of Li nanoclusters suggests that the second model is more adequate. Therefore, it is suggested that the LiCl-Li₂O-Li electrolyte is a complex solution consisting of at least two phases; Li dissolved in LiCl-Li₂O, and a dispersed Li rich phase.

LiCl-Li₂O-Li and the Reduction of Actinide Oxides

Evidence of the presence of elemental lithium in the electrolyte during the electrolytic reduction process includes the coloring of the molten salt from the formation of "metal fog", dark purple ribbons in the relatively transparent LiCl-Li₂O solution, and the bubbling of salt samples upon contact with water.^{115,117-119} These observations, along with the low current efficiencies reported throughout the electrolytic reduction literature, are indicative of the presence of metal-salt solutions, and similar to the observations that led their study in the first half of the 20th century.^{89,90,92,94} As will be shown in the following examples, the generation of a complex LiCl-Li₂O-Li electrolyte during the reduction of actinide oxides has significant implications regarding the oxide reduction process.

A method of electrochemically recycling metallic Li throughout successive UO₂ reduction runs has been developed specifically to control the excess Li that accumulates in the cathode assembly.⁷⁷ This investigation noted that the accumulation of excess Li in the cathode assembly could be detrimental to post reduction processes such as salt vaporization and electrorefining. In these experiments a typical reduction run of UO₂ was completed by passing 190% of the theoretical charge through the electrolytic reduction cell for the given quantity of UO₂. The reduced U cathode assembly that contained excess Li was then polarized as the anode against a stainless steel rod at +0.3 V; to oxidize the Li from the metallic U deposit and reduce Li⁺ at the stainless steel rod. The deposited Li was then used as a reducing agent in the reduction of a new batch of UO₂, were it reacted chemically with the UO₂ to regenerate the Li₂O lost in the initial UO₂ reduction run. This study successfully demonstrated all of these steps in succession, and proved that excess Li could be recycled in subsequent electrolytic reductions of UO₂. It is important to note however, that Park et al. stated numerous times that the electrolyte was saturated with Li and that losses of charge transfer, along with Li and Li₂O, occurred during the separate stages of the recycling process.

Alternatively, Herrmann et al. have employed a secondary circuit to oxidize Li prior to its dissolution in an attempt to suppress Li attack of the Pt anode.^{42,75,76,120} A power supply was connected between the cathode lead, a stainless steel rod at the center of the cathode, and the exterior of the stainless steel basket of the cathode assembly. This power supply was energized in a galvanostatic mode when the cathode lead approached the Li|Li⁺ potential. The current passed through this secondary power supply, I-sec, the potential of the basket wall, V-BW,

and the potential of the cathode lead, V-CL, are shown in Figure 2e. Although the basket wall is maintained at a positive potential with respect to the cathode lead, it is observed that the OCP of both exhibit the Li|Li⁺ potential during the cell interruption at the end of the experiment. No quantitative information regarding the success of this configuration in the containment of Li could be found in the published literature, however it was noted that the 1 mm diameter Pt wire anode was used in six successive reduction runs without exhibiting extensive corrosion.⁷⁶

The generation of excess Li during the reduction process could result in decreased current efficiencies by several mechanisms. The reduction of Li⁺ consumes an electron and as a result the consumption of Li by any mechanism other than the reduction of actinide oxides leads to a loss in process efficiency. First, dissolved Li can recombine with O_{2(g)} prior to complete evolution resulting in the regeneration of Li₂O. Secondly, dissolved Li can react with materials exposed to the melt such as Al₂O₃ or MgO. Additionally, while the solubility limit of Li is low when considered as a weight percent, the dissolution of even 0.1 wt% Li into a multi kilogram LiCl electrolyte is large on a mol basis. As a result, the generation of a LiCl electrolyte that is saturated with Li requires the consumption of a notable amount of the charge passed through the cell. Finally, when Li is present in the electrolyte, the resulting metal-salt solution exhibits electron conduction in addition to ion migration as a mechanism of charge transfer. Any charged passed through the electrochemical cell that is carried by electrons will not contribute to the reduction of actinide oxides and is therefore considered a loss.

Quantification of the concentration of Li in the electrolyte during the electrolytic reduction process could be used to evaluate these inefficiencies, however two technical difficulties exist in quantifying the concentration of Li in melts of LiCl-Li₂O-Li. First, the concentration of Li₂O in samples of the electrolyte is commonly quantified by titrating a sample of the salt; assuming that Li₂O in the salt reacts with water to produce basic LiOH. However, if Li is present in the salt sample as well, it will react with water to form H_{2(g)} and LiOH. As a result, careful analysis of the quantity of H_{2(g)} that results from contacting a sample of the electrolyte with water must be taken into account, and the quantity of LiOH that results from the presence of Li must then be subtracted from the titration measurement. Unfortunately, numerous researchers have employed such a titration methodology without explicitly stating that H_{2(g)} evolution was accounted for.^{4-6,43,77} As a result, it is difficult to quantify to what degree these measurements are accurate. The technical difficulties associated with quantifying the production of H_{2(g)} and discerning the correct concentration of Li₂O have been previously emphasized.^{98,121} Furthermore, the validity of salt sampling techniques based on freezing salt on a dipstick is questionable due to the highly temperature dependent phase stability of LiCl-Li solutions.^{79,81}

The second difficulty in quantifying the degree to which Li is present in the LiCl-Li₂O electrolyte is that Li is known to react with nearly all molecular compounds, many of which are frequently in contact with the electrolyte during the reduction process. Dworkin et al. first noted that LiCl-Li was observed to react with, and physically degrade, both synthetic sapphire and single crystal MgO.⁷⁹ Commercial grade MgO is widely employed as a crucible material and as an electrode shroud in the oxide reduction process.^{45,85} Significantly, recent research by Choi et al. into the development of anode shrouds noted degradation of MgO during the reduction of UO₂.⁴⁵ Figure 5 shows two anode shrouds fabricated of MgO and MgO (3 wt%)-ZrO₂ before and after being used to reduce UO₂ in LiCl-Li₂O. Considering the physical separation of the anode shroud and the cathode assembly, the degradation of the materials was attributed to reactions with Li dissolved in the electrolyte.

MgO-ZrO₂ coated stainless steel mesh (STS) was investigated as an alternative anode shroud material.⁴⁵ As shown in Figure 6, MgO-ZrO₂ coated STS was shown to be stable when exposed to molten LiCl-Li₂O at 650°C over the course of 21 days; however, it was found to be severely degraded when employed as the anode shroud during the electrolytic reduction of 20 g of UO₂ over the course of 1.5 hours. The

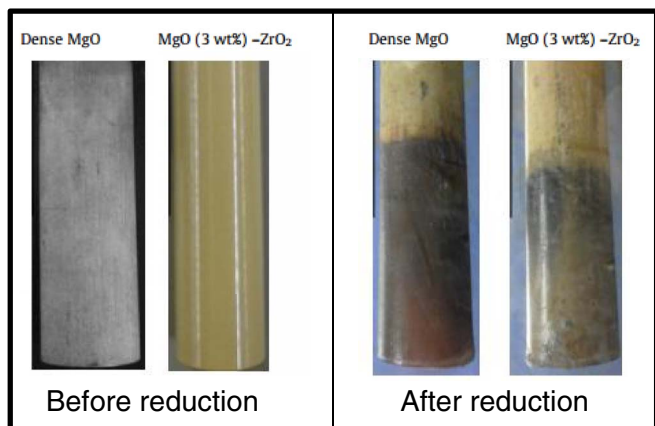


Figure 5. MgO and MgO (3 wt%)–ZrO₂ anode shrouds before and after being employed for reducing UO₂ in LiCl–Li₂O at 650°C. The visible degradation was attributed to chemical attack by dissolved Li in the electrolyte.⁴⁵

degradation that occurred when the material was employed as an anode shroud, and not during the extended period of exposure, was attributed to the accumulation of Li in the electrolyte during the reduction of UO₂. Similar degradation was reported when MgO–ZrO₂ coated STS was exposed to LiCl–Li₂O containing 0.3 wt% (~2 mol%)Li. Interestingly, the authors noted explicitly that the degradation resulting from exposure to the LiCl–Li₂O–0.3 wt% Li solution was similar to the damage experienced during the reduction run, however the data were not provided. These observations suggest that Li disperses into the electrolyte during the reduction process up to concentrations exceeding the physical solubility limit. The rate at which LiCl–Li₂O–Li reacts with MgO is currently unknown, and as a result it is impossible to suggest to what degree Li is consumed by MgO throughout the electrolytic reduction process. The reaction of dissolved Li and MgO is suggested to be a significant loss of current efficiency and a source of experimental error in numerous reports; specifically, those employing MgO crucibles.

Lithium has been recovered from molten LiCl–Li₂O by reducing Li⁺ at a cathode inside a porous MgO shroud.³¹ After accumulating Li in the cathode container, the container was lifted out of the melt and the Li was extracted using a vacuum syphon. It was suggested that the fluid salt drained from the porous ceramic while the Li was contained inside the MgO. It was reported that greater than 95% of

the reduced Li was recovered using this method; however, this study falls victim to the previously mentioned experimental uncertainties associated with quantification of the concentration of Li and Li₂O in molten LiCl. Furthermore, the containment of reasonably pure Li in MgO is questionable due to the chemical reactivity of liquid Li. If present as a colloid in the electrolyte, metallic lithium is known to react spontaneously with nearly all commercial ceramics.¹²²

The stability of yttria-stabilized zirconia (YSZ) in molten LiCl–Li₂O–Li has been investigated.¹²³ YSZ was observed to be stable upon static exposure to molten LiCl–Li₂O containing 0.036 wt%Li. However, it was noted that when the material was in contact with a cathode used to reduce UO₂ in LiCl–Li₂O, the surface of the material was found to have reduced to Zr metal.¹²³ Alternative studies have reported Li dispersed in LiCl–Li₂O to degrade YSZ.¹²⁴ The reduction of ZrO₂ in molten LiCl–Li₂O has been studied due to the relevance of ZrO₂ to nuclear fuel processing. It was noted that incomplete reduction occurred when ZrO₂ was subjected to electrolytic reduction in LiCl–Li₂O.¹²⁵ Lithium zirconate (Li₂ZrO₃) formed when the process was conducted in LiCl–1 wt%Li₂O, and zirconates possessing a higher ratio of Li₂O to ZrO₂ formed when the material was reduced in melts containing higher concentrations of Li₂O.

Sakamura et al. noted that the current efficiency of the oxide reduction process decreased and the Li₂O loss rate increased when a cathode assembly was rotated during reduction.⁵ This observation was attributed to the agitation of the electrolyte causing accelerated dissolution of Li from the cathode. Similar phenomena were reported by INL where consistent Li₂O concentrations were recorded for a number of reduction runs that employed stationary electrodes, but became less repeatable, and with greater losses of Li₂O, when the cathode basket was rotated.⁴⁷ Further investigations into these effects are suggested to suppress losses of current efficiency and Li₂O consumption.

Simpson et al. were successful in modeling literature data on the kinetics of the lithium reduction process, not electrochemically driven, using a shrinking core model of the UO₂ pellets by employing literature data of the Li solubility limit as 1.7×10^{-4} mol/cm³ (~0.5 mol%).^{86,126} This report explicitly stated that the diffusivity of the melt in the porous uranium metal was found to be exceedingly high at 9.7×10^{-4} cm²/s, and suggested that the concentration of lithium in the salt might have been significantly greater than the solubility limit implied. Subsequent modeling of the electrolytic reduction process, also conducted by INL, reported an effective diffusion coefficient considerably closer to analogous systems by employing a higher concentration of lithium in the salt, citing the solubility limit as 0.0058 g/cm³ (~2.3

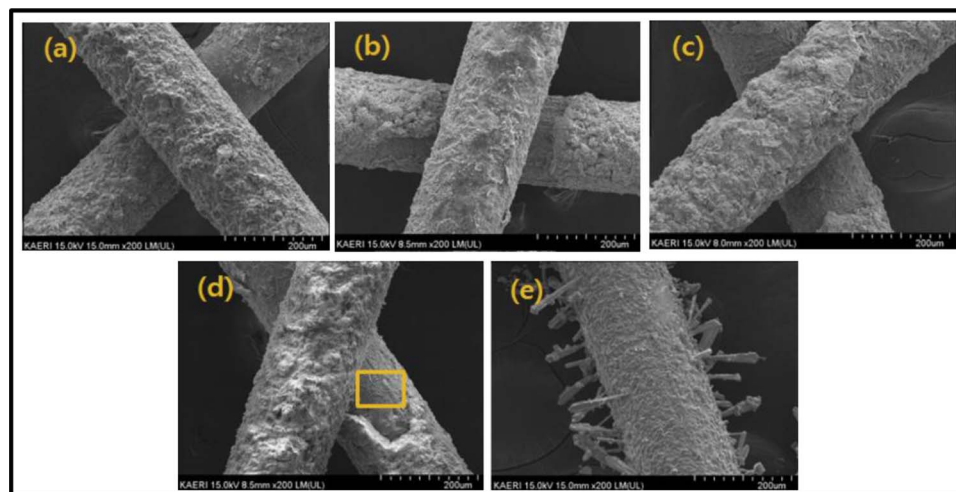


Figure 6. SEM micrographs of MgO–ZrO₂ coated STS meshes (a) original, and exposed to LiCl–Li₂O at 650°C for (b) 7 days, (c) 14 days, (d) 21 days, and (e) after being employed as an anode shroud during the electrolytic reduction of 20 g of UO₂ over the course of 1.5 hours. The damage to the ceramic coatings of the steel shown in (e), and not as a result of extended period of exposure, was attributed to the presence of Li in the molten salt accumulated during the operation of the reduction cell.⁴⁵

mol%).⁴⁶ This value is in agreement with the higher concentrations of dispersed lithium previously discussed, however the origin of this solubility limit could not be found in the cited reference by Park et al.⁴³ While the adaptation of diffusion limited kinetic models has been shown to be effective in predicting process kinetics, the inconsistency in the values of lithium concentration employed should be further investigated.

The accumulation of excess Li has been stated to coincide with a loss of Li₂O as a result of the continued electrolysis of Li₂O after the intended reduction of the actinide oxides, due to the inability of the operator to know when the reduction of the actinide oxide is complete.⁷⁷ This conclusion is suspect however, as the depletion of Li₂O has been observed to be continuous throughout the reduction process.^{47,69} The reported rates of Li₂O consumption during the reduction process vary widely between references; an inconsistency that is attributed to the previously mentioned difficulties in quantifying the concentration of Li and Li₂O in the salt, the quantity of Li that is lost to side reactions, and the quantity of Li and Li₂O that remain in the cathode basket.^{6,42,72,84,127} Furthermore, the concentration of Li₂O in the electrolyte can be diminished if the rate of O²⁻ oxidation at the anode exceeds the transport of O²⁻ from the UO₂ out of the cathode assembly. Continued oxidation of O²⁻ at a greater rate than the electrolyte can be replenished from the reduction of UO₂ would result in the direct electrolysis of Li₂O without inducing the reduction of further UO₂.

The final aspect of the role of lithium in the electrolytic reduction of actinide oxides to be discussed is the underpotential deposition (UPD) of Li⁺. UPD is the formation of single monolayers of atoms on a foreign substrate at a potential more noble than is required to reduce successive bulk metal onto the initial monolayer.¹²⁸⁻¹³¹ The UPD of Li⁺ from molten LiCl has been reported to occur on the surface of U₃O₈ as well as numerous other substrates.^{24,132-134} Application of modern theory of UPD is beyond the scope of this review; however, it is illuminating to note the following basic effects. UPD occurs when the binding energy between a deposited species and a substrate is greater than the binding energy of the pure metallic species. As a result, there is an energetic benefit to the deposition of a monolayer of metal onto the foreign material compared to the subsequent reduction of the species onto like atoms. This effect manifests itself in a thermodynamic activity of the reduced metal being less than unity as long as the foreign substrate is exposed. As predicted by the Nernst equation, this results in the first monolayer being deposited at a more noble electrochemical potential.

While the UPD of Li⁺ from LiCl-Li₂O has been shown to occur on U₃O₈, it was explicitly not observed on a Ni wire in the same study.¹³⁴ Numerous alternative CV's of metal electrodes in LiCl-Li₂O have also not detected any UPD current.^{68,75,135} It has been demonstrated that the activity of Li in LiCl is significantly less than unity, even under Li saturated conditions.⁸¹ This observation is highly supportive of the feasibility of Li⁺ UPD, as it would raise the Li|Li⁺ reduction potential. Similar low activity behavior of Li in LiCl was reported when investigating the deposition and intercalation of Li from LiCl into graphite.¹³³ This work is of specific interest as the authors noted that both the kinetics of Li deposition, and the reduction potential itself, were highly dependent upon the porosity of the graphite substrate. This effect could play an analogous role in the UPD of Li⁺ on porous uranium oxides.

Despite these observations, the UPD of Li⁺ on U₃O₈ is interesting because metallic Li reacts spontaneously with U₃O₈.⁴³ In order for UPD of Li⁺ to occur on the surface of U₃O₈, an electron would be required to transport through the U₃O₈ to the electrolyte interface, and reduce the Li⁺ ion. This is exceedingly unlikely as the reduction potential of U₃O₈ is more noble than that of Li⁺. If this process were to occur, the recently formed Li would then immediately react with the U₃O₈. Significant theoretical difficulties exist in this respect due to the non-unit activity of Li in LiCl and the complex valance structure of U₃O₈ as well as intermediately reduced lithium uranates. Therefore, it is probably not accurate to discuss reduction of Li⁺ at U₃O₈ in terms of UPD. Further investigations, both theoretical and experi-

mental, are required before an understanding of these effects can be presented.

Summary

Metallic lithium is inevitably formed during the electrolytic reduction of actinide oxides in LiCl-Li₂O. Polarization of the cathode below the reduction potential of Li⁺ is required to facilitate efficient and high yield reductions. As a result, metallic lithium is deposited on the cathode basket throughout the reduction process. Li has been observed to be in physical contact with the cathode and the molten LiCl-Li₂O electrolyte. The solubility of Li in molten LiCl-Li₂O is well documented, and yet the amount of Li that disperses into the electrolyte during the reduction process has not been quantified. Dispersion of Li in molten LiCl is reported to occur via multiple possible mechanisms: true physical dissolution, the formation of subhalide complexes, and colloidal suspension as nanoclusters. The true dissolution of Li in LiCl appears to have a solubility limit of ~0.5 mol%, while the limit of dispersion may not be well defined.

The effect of the generation of a LiCl-Li₂O-Li electrolyte on the electrolytic reduction process is not known due to the experimental difficulties associated with isolation of potential variables. It is suggested that dispersed Li is a likely cause for the reported low current efficiencies of the process due to recombination of Li with oxygen to form Li₂O. Additionally, the loss of Li dissolved into the electrolyte as well as via reactions with unintended materials represents a possible consumption mechanism of Li₂O and electric charge. The degradation of ceramic materials exposed to the electrolyte, notably MgO, have been reported to occur due to the presence of dispersed Li, however the reaction rates associated with the consumption of Li are yet unknown. Further research regarding these effects is essential to understand the role of lithium in the electrolytic reduction of actinide oxides.

Acknowledgments

This work was supported by the Department of Energy (DOE) under award DE-NE0008262 and the Nuclear Regulatory Commission (NRC) under awards NRC-HQ-11-G-38-0039 and NRC-38-10-949. A.M. is supported under NRC Fellowship award. Kenny Osborne serves as the program manager for the DOE award. Nancy Hebron-Isreal serves as the grants program officer for the NRC awards.

References

1. T. Nakajima, K. Nakanishi, and N. Watanabe, *Bull. Chem. Soc. Jpn.*, **49**, 994 (1975).
2. J. J. Laidler, J. E. Battles, W. E. Miller, J. P. Ackerman, and E. L. Carls, *Prog. Nucl. Energy*, **31**, 131 (1997).
3. T. Inoue and L. Koch, *Nucl. Eng. Technol.*, **4**, 183 (2008).
4. Y. Sakamura, *J. Nucl. Mater.*, **412**, 177 (2011).
5. Y. Sakamura, T. Omori, and T. Inoue, *Nucl. Technol.*, 162 (2007).
6. S. M. Jeong, S. B. Park, S. S. Hong, C. S. Seo, and S. W. Park, *J. Radioanal. Nucl. Chem.*, **268**, 349 (2006).
7. E.-Y. Choi, J.-M. Hur, I.-K. Choi, S. G. Kwon, D.-S. Kang, S. S. Hong, H.-S. Shin, M. A. Yoo, and S. M. Jeong, *J. Nucl. Mater.*, **418**, 87 (2011).
8. S. D. Herrmann, S. X. Li, and B. R. Westphal, *Sep. Sci. Technol.*, **47**, 2044 (2012).
9. H. Lee in, *Reprocessing and Recycling of Spent Nuclear Fuel*, p. 415, Woodhead Publishing, Oxford (2015).
10. T. M. Besmann and R. H. J. Cooper, Chemical thermodynamic assessment of the Li-U-O system for possible space nuclear applications, Oak Ridge National Laboratory, Report ORNL/TM-9662 (1985).
11. E. Karell, R. Pierce, and T. Mulcahey, Treatment of oxide spent fuel using the lithium reduction process, in, Argonne National Laboratory, Report ANL-CMT/CP-89562 (1996).
12. J. L. Willit, W. E. Miller, and J. E. Battles, *J. Nucl. Mater.*, **195**, 229 (1992).
13. L. I. Redey and K. Gourishankar, Direct electrochemical reduction of metal-oxides, US Patent: 6,540,902 B1 (2001).
14. D. S. Poa, L. Burris, R. K. Steunenber, and Z. Tomczuk, Apparatus and Process for the Electrolytic Reduction of Uranium and Plutonium Oxides, US Patent: 4,995,948 (1991).
15. J. J. Laidler, Chemical Technology Division Annual Technical Report, p. 97, and Argonne National Laboratory Report ANL-96/10, (1995).

16. K. V. Gourishankar, E. R. Karell, R. E. Everhart, and E. Indacochea, in *Embedded Topical Meeting on DOE Spent Nuclear Fuel and Fissile Material Management*, p. 65, San Diego, CA (2000).
17. E. J. Karell, K. V. Gourishankar, L. S. Chow, and R. E. Everhart, in *Global '99: "Nuclear Technology - Bridging the Millennia"*, p. 78, Jackson Hole, WY (1999).
18. E. Karell, K. Gourishankar, J. Smith, L. Chow, and L. Redey, *Nucl. Technol.*, **136**, 343 (2001).
19. E. J. Karell and K. V. Gourishankar, in *Third Topical Meeting on DOE Spent Nuclear Fuel and Fissile Materials Management*, T. A. N. Society Editor, p. 682, Charleston, SC (1998).
20. K. Gourishankar, L. Redey, and M. Williamson, in *Light Metals*, p. 1075 (2002).
21. G. Z. Chen, D. J. Fray, and T. W. Farthing, *Nature*, **407**, 361 (2000).
22. D. Fray, T. Farthing, and Z. Chen, Removal of oxygen from metal oxides and solid solutions by electrolysis in a fused salt. International Patent: US 20040159559 A1 (1999).
23. A. M. Abdelkader, K. T. Kilby, A. Cox, and D. J. Fray, *Chem. Rev. (Washington, DC, U. S.)*, **113**, 2863 (2013).
24. W. Xiao and D. Wang, *Chem. Soc. Rev.*, **43**, 3215 (2014).
25. K. S. Mohandas, *Mineral Proc. Extractive Metall.*, **122**, 195 (2013).
26. E.-Y. Choi and S. M. Jeong, *Prog. Nat. Sc.: Mater. Intl.*, **25**, 572 (2015).
27. Y. Sakamura, *J. Electrochem. Soc.*, **157**, E135 (2010).
28. Y. Kado, T. Goto, and R. Hagiwara, *J. Chem. Eng. Data*, **53**, 2816 (2008).
29. T. Usami, M. Kurata, T. Inoue, H. E. Sims, S. A. Beetham, and J. A. Jenkins, *J. Nucl. Mater.*, **300**, 15 (2002).
30. B. Park, S. Park, S. Jeong, C. Seo, and S. Park, *J. Radioanal. Nucl. Chem.*, **270**, 575 (2006).
31. J. Hur, C. Seo, S. Hong, D. Kang, and S. Park, *J. Korean, Radioactive Waste Soc.*, **2**, 211 (2004).
32. T. Usami, T. Kato, M. Kurata, T. Inoue, H. E. Sims, S. A. Beetham, and J. A. Jenkins, *J. Nucl. Mater.*, **304**, 50 (2002).
33. S. Jeong, J. Hur, S. Hong, D. Kang, M. Choung, X. Seo, J. Yoon, and S. Park, *Nucl. Technol.*, **162**, 184 (2007).
34. M. Kurata, T. Inoue, J. Serp, M. Ougier, and J.-P. Glatz, *J. Nucl. Mater.*, **328**, 97 (2004).
35. E.-Y. Choi, J. W. Lee, J. J. Park, J.-M. Hur, J.-K. Kim, K. Y. Jung, and S. M. Jeong, *Chem. Eng. J. (Lausanne)*, **207-208**, 514 (2012).
36. W. Park, E.-Y. Choi, S.-W. Kim, S.-C. Jeon, Y.-H. Cho, and J.-M. Hur, *J. Nucl. Mater.*, **477**, 59 (2016).
37. J.-M. Hur, S.-C. Lee, S.-M. Jeong, and C.-S. Seo, *Chem. Lett.*, **36**, 1028 (2007).
38. S.-C. Lee, J.-M. Hur, and C.-S. Seo, *J. Ind. Eng. Chem.*, **14**, 651 (2008).
39. S. M. Jeong, J.-Y. Jung, C.-S. Seo, and S.-W. Park, *J. Alloys Compd.*, **440**, 210 (2007).
40. S. M. Jeong, H. Y. Yoo, J.-M. Hur, and C.-S. Seo, *J. Alloys Compd.*, **452**, 27 (2008).
41. Chemical Reaction and Equilibrium Software with Extensive Thermochemical Database, Version 5.1, HSC Chemistry (2002).
42. S. Herrmann, S. Li, and M. Simpson, *J. Nucl. Sci. Technol.*, **44**, 361 (2007).
43. B. H. Park, I. W. Lee, and C. S. Seo, *Chem. Eng. Sci.*, **63**, 3485 (2008).
44. J.-M. Hur, C.-S. Seo, S.-S. Hong, D.-S. Kang, and S.-W. Park, *React. Kinet. Catal. Lett.*, **80**, 217 (2003).
45. E.-Y. Choi, C. Y. Won, J.-S. Cha, W. Park, H. S. Im, S.-S. Hong, and J.-M. Hur, *J. Nucl. Mater.*, **444**, 261 (2014).
46. S. Phongikaroon, S. Herrmann, and M. Simpson, *Nucl. Technol.*, **174** (2010).
47. S. Herrmann, S. Li, and B. Serrano-Rodriguez, Observations of Oxygen Ion Behavior in the Lithium-Based Electrolytic Reduction of Uranium Oxide in GLOBAL 2009, American Nuclear Society (2009).
48. W. Park, J.-K. Kim, J.-M. Hur, E.-Y. Choi, H. S. Im, and S.-S. Hong, *J. Nucl. Mater.*, **432**, 175 (2013).
49. Y. Sakamura, *Electrochim. Acta*, **80**, 308 (2012).
50. T. B. Joseph, N. Sanil, L. Shakila, K. S. Mohandas, and K. Nagarajan, *Electrochim. Acta*, **139**, 394 (2014).
51. S. M. Jeong, H.-S. Shin, S.-H. Cho, J.-M. Hur, and H. S. Lee, *Electrochim. Acta*, **54**, 6335 (2009).
52. J. M. Hur, J. Cha, and E. Y. Choi, *ECS Electrochem. Lett.*, **3**, E5 (2014).
53. A. Merwin and D. Chidambaram, *Metall. Trans. A*, **46**, 536 (2015).
54. P. Motsegood, Development of Carbon Anodes for Use in Electrolytic Reduction of Used Oxide Fuel, in *International Pyroprocessing Research Conference*, Idaho Falls, ID (2014).
55. S.-W. Kim, M. K. Jeon, H. W. Kang, S.-K. Lee, E.-Y. Choi, W. Park, S.-S. Hong, S.-C. Oh, and J.-M. Hur, *J. Radioanal. Nucl. Chem.*, **310**, 463 (2016).
56. S.-W. Kim, E.-Y. Choi, W. Park, H. S. Im, and J.-M. Hur, *Electrochem. Comm.*, **55**, 14 (2015).
57. S.-W. Kim, E.-Y. Choi, W. Park, H. S. Im, and J.-M. Hur, *J. Nucl. Fuel Cycle and Waste Tech. (JNFCWT)*, **13**, 229 (2015).
58. S.-W. Kim, H. W. Kang, M. K. Jeon, S.-K. Lee, E.-Y. Choi, W. Park, S.-S. Hong, S.-C. Oh, and J.-M. Hur, *Nucl. Eng. Tech.*, **48**, 997 (2016).
59. Y. Sakamura and M. Iizuka, *Electrochim. Acta*, **189**, 74 (2016).
60. M. K. Yoshiharu Sakamura and Tadashi Inoue, *J. Electrochem. Soc.*, **153**(3) (2006).
61. W. I. Ko, H. H. Lee, S. Choi, S.-K. Kim, B. H. Park, H. J. Lee, I. T. Kim, and H. S. Lee, *Nucl. Eng. Des.*, **277**, 212 (2014).
62. J. Park, I. Jung, and J. Shin, Development of Voloxidation Process for Treatment of LWR spent Fuel, Korea Atomic Energy Research Institute, Report KAERI/RR-2841/2006 (2007).
63. B. P. Westphal, K. J. Bateman, C. D. Morgan, J. F. Berg, P. J. Crane, D. G. Cummings, J. J. Giglio, M. W. Huntley, R. P. Lind, and D. A. Sell, *Nucl. Technol.*, **162**, 153 (2008).
64. M. F. Simpson, Development of Spent Nuclear Fuel Reprocessing Technology, Idaho National Laboratory, Document INL/EXT-12-25124 (2012).
65. K. C. Song, G. I. Park, J. W. Lee, J. J. Park, and M. S. Yang, *Nucl. Technol.*, **162**, 158 (2008).
66. E.-Y. Choi, J.-K. Kim, H.-S. Im, I.-K. Choi, S.-H. Na, J. W. Lee, S. M. Jeong, and J.-M. Hur, *J. Nucl. Mater.*, **437**, 178 (2013).
67. B. H. Park, I. W. Lee, and C.-S. Seo, *J. Chem. Eng. Jpn.*, **41**, 294 (2008).
68. S. M. Jeong, H.-S. Shin, S.-S. Hong, J.-M. Hur, J. B. Do, and H. S. Lee, *Electrochim. Acta*, **55**, 1749 (2010).
69. J.-M. Hur, I.-K. Choi, S.-H. Cho, S.-M. Jeong, and C.-S. Seo, *J. Alloys Compd.*, **452**, 23 (2008).
70. Y. Sakamura and T. Omori, *Nucl. Technol.*, **171**, 266 (2010).
71. Y. Sakamura, *Nucl. Technol.*, **179**, 220 (2012).
72. J.-M. Hur, S.-S. Hong, and H. Lee, *J. Radioanal. Nucl. Chem.*, **295**, 851 (2013).
73. E.-Y. Choi, C. Y. Won, S.-J. Lee, D.-S. Kang, S.-W. Kim, J.-S. Cha, W. Park, H. S. Im, and J.-M. Hur, *Ann. Nucl. Energy*, **76**, 305 (2015).
74. E. Choi, H. Im, and J. Hur, *J. Korean Electrochem. Soc.*, **16**, 138 (2013).
75. S. Herrmann, S. Li, M. Simpson, and S. Phongikaroon, *Sep. Sc. Tech.*, **41**, 1965 (2006).
76. S. Herrmann and S. Li, *Nucl. Technol.*, **171**, 247 (2010).
77. W. Park, J.-M. Hur, S.-S. Hong, E.-Y. Choi, H. S. Im, S.-C. Oh, and J.-W. Lee, *J. Nucl. Mater.*, **441**, 232 (2013).
78. M. Iizuka, Y. Sakamura, and T. Inoue, *J. Nucl. Mater.*, **359**, 102 (2006).
79. A. S. Dworkin, H. R. Bronstein, and M. A. Bredig, *J. Phys. Chem.*, **66**, 572 (1962).
80. J. Liu and J. C. Poignet, *J. Appl. Electrochem.*, **22**, 1110 (1992).
81. J. Liu and J. C. Poignet, *J. Appl. Electrochem.*, **20**, 864 (1990).
82. T. Nakajima, K. Nakanishi, and N. Watanabe, *Nippon Kagaku Kaishi*, **1975**, 617 (1975).
83. N. Watanabe, K. Nakanishi, and T. Nakajima, *Nippon Kagaku Kaishi*, **1974**, 401 (1974).
84. S. Herrmann, S. Li, and B. Westphal, Separation and Recovery of Uranium and Group Actinide Products from Irradiated Fast Reactor MOX Fuel via Electrolytic Reduction and Electrorefining, in *3rd International Pyroprocessing Research Conference*, Dimitrovgrad, Russia (2010).
85. S. Herrmann and S. Li, *Nucl. Technol.*, **171**, 247 (2010).
86. M. Simpson and S. Herrmann, *Nucl. Technol.*, **162**, 179 (2008).
87. P. Kar and J. W. Evans, *Electrochim. Acta*, **53**, 5260 (2008).
88. P. Kar and J. W. Evans, *Electrochim. Acta*, **54**, 835 (2008).
89. M. A. Bredig, in *Molten Salt Chemistry*, J. W. a. Sons Editor (1964).
90. G. M. Haarberg and J. Thonstad, *J. Appl. Electrochem.*, **19**, 789 (1989).
91. J. D. Corbett, The Solutions of Metals in their Molten Salts, in *Fused Salts*, McGraw Hill (1964).
92. J. W. Warren, Electronic Properties of Metal / Molten Salt Solutions, in *Molten Salts: From Fundamentals to Applications*, Editor: M. Gaune-Escard, Kluwer Academic Publishers (2001).
93. H. R. Bronstein and M. A. Bredig, *J. Am. Chem. Soc.*, **80**, 2077 (1958).
94. W. W. Warren, *Metal-Metal Salt Solutions*, in *Advanced Molten Salt Chemistry*, Reidel Publishing (1983).
95. W. Freyland, *J. Non-Cryst. Solids*, **117**, 613 (1990).
96. L. F. Grantham and S. J. Yosim, *J. Chem. Phys.*, **38**, 1671 (1963).
97. P. Héban and G. S. Picard, *Electrochim. Acta*, **43**, 2071 (1998).
98. A. J. Burak and M. F. Simpson, *J. Met.*, **68**, 2639 (2016).
99. A. S. Dworkin and M. A. Bredig, *J. Phys. Chem.*, **74**, 3828 (1970).
100. M. A. Bredig and H. R. Bronstein, *J. Phys. Chem.*, **64**, 64 (1960).
101. A. S. Dworkin, H. R. Bronstein, and M. A. Bredig, *J. Phys. Chem.*, **72**, 1892 (1968).
102. T. Nakajima, R. Minami, K. Nakanishi, and N. Watanabe, *Bull. Chem. Soc. Jpn.*, **47**, 2071 (1974).
103. H. Moriyama, T. Nagae, and Y. Ito, *J. Nucl. Mater.*, **211**, 231 (1994).
104. K. Chang and B. Hallstedt, *Calphad*, **35**, 160 (2011).
105. P. Héban and G. S. Picard, *J. Mol. Str.: THEOCHEM*, **426**, 225 (1998).
106. R. O. Jones, A. I. Lichtenstein, and J. Hutter, *J. Chem. Phys.*, **106**, 4566 (1997).
107. C. H. Wu, H. Kudo, and H. R. Ihle, *J. Chem. Phys.*, **70**, 1815 (1979).
108. H. Kudo and K. Yokoyama, *Bull. Chem. Soc. Jpn.*, **69**, 1459 (1996).
109. S. Neukermans, E. Janssens, H. Tanaka, R. E. Silverans, P. Lievens, K. Yokoyama, and H. Kudo, *J. Chem. Phys.*, **119**, 7206 (2003).
110. M. Gutowski and J. Simons, *J. Phys. Chem.*, **98**, 8326 (1994).
111. S. Zein and J. V. Ortiz, *The J. Chem. Phys.*, **135** (2011).
112. V. L. Cherginet, *Electrochim. Acta*, **42**, 1507 (1997).
113. M. P. Tosi, *J. Mater. Sci. Technol.*, **14** (1998).
114. P. Masset and R. A. Guidotti, *J. Power Sources*, **164**, 397 (2007).
115. T. Takenaka, K. Shigeta, H. Masuhama, and K. Kubota, *ECS Trans.*, **49**, 441 (2009).
116. A. Merwin, W. Phillips, M. A. Williamson, J. Willit, P. N. Motsegood, and D. Chidambaram, *Sci. Rep.*, **6**, 25435 (2016).
117. N. Gese and B. Pesic, Electrochemistry of LiCl-Li₂O-H₂O Molten Salt Systems, in *2013 TMS Annual Meeting & Exhibition*, TMS (2013).
118. S. M. Jeong, B. H. Park, J.-i.-m. Hur, C.-S. Seo, H. Lee, and K.-C. Song, *Nucl. Eng. Technol.*, **42**, 183 (2010).
119. T. Takenaka, T. Morishige, and M. Umehara, Cathodic Phenomena in Li Electrolysis in LiCl-KCl Melt, in *Molten Salts Chemistry and Technology*, p. 143, John Wiley & Sons, Ltd (2014).
120. S. Herrmann, S. Li, and M. Simpson, Electrolytic Reduction of Spent Oxide Fuel – Bench-Scale Test Results, in *GLOBAL 2005* (2005).
121. I. K. Choi, Y. H. Cho, J. W. Yeon, W. Kim, and T. J. Kim, Measuring the conversion yield of uranium by electrochemical analysis based on an oxidation of an oxygen ion and a reduction of a lithium ion dissociated from lithium oxide obtained

- as a by-product; electrical measuring instruments, US Patent: US7,390,392 B1 (2008).
122. D. W. Jeppson, J. L. Ballif, W. W. Yuan, and B. E. Chou, Lithium Literature Review: Lithium's Properties and Interactions, in Hanford Engineering Development Laboratory Report HEDL-TME 78-15 (1978).
 123. E.-Y. Choi, J. Lee, S.-J. Lee, S.-W. Kim, S.-C. Jeon, S. H. Cho, S. C. Oh, M. K. Jeon, S. K. Lee, H. W. Kang, and J.-M. Hur, *J. Nucl. Mater.*, **475**, 57 (2016).
 124. T.-J. Kim, Y.-H. Cho, I.-K. Choi, J.-G. Kang, K. Song, and K.-Y. Jee, *J. Nucl. Mater.*, **375**, 275 (2008).
 125. Y. Sakamura, M. Iizuka, S. Kitawaki, A. Nakayoshi, and H. Kofuji, *J. Nucl. Mater.*, **466**, 269 (2015).
 126. E. R. Van Artsdalen and I. S. Yaffe, *J. Phy. Chem.*, **59**, 118 (1955).
 127. M. Simpson, Developments of Spent Nuclear Fuel Pyroprocessing Technology, Idaho National Laboratory, Report INL/EXT-12-25124 (2012).
 128. D. M. Kolb, M. Przasnyski, and H. Gerischer, *J. Electroanal. Chem. Interfacial Electrochem.*, **54**, 25 (1974).
 129. G. Kokkinidis, *J. Electroanal. Chem. Interfacial Electrochem.*, **201**, 217 (1986).
 130. D. M. Kolb and H. Gerischer, *Surf. Sci.*, **51**, 323 (1975).
 131. O. A. Oviedo, P. Vélez, V. A. Macagno, and E. P. M. Leiva, *Surf. Sci.*, **631**, 23 (2015).
 132. Y. Xue, Y. Yan, M. Zhang, W. Han, and Z. Zhang, *J. Rare Earths*, **30**, 1048 (2012).
 133. Q. Xu, C. Schwandt, G. Z. Chen, and D. J. Fray, *J. Electroanal. Chem.*, **530**, 16 (2002).
 134. J.-M. Hur, S. M. Jeong, and H. Lee, *Electrochem. Commun.*, **12**, 706 (2010).
 135. S. Herrmann, S. Li, D. Sell, and B. Westphal, Electrolytic Reduction of Spent Nuclear Oxide Fuel – Effects of Fuel Form and Cathode Containment Materials on Bench-Scale Operations, Idaho National Laboratory Report INL/CON-07-12182 (2007).